

## PAPER

[View Article Online](#)  
[View Journal](#) | [View Issue](#)


Cite this: *Food Funct.*, 2022, **13**, 11715

# Genistein improves glucose metabolism and promotes adipose tissue browning through modulating gut microbiota in mice†

Shunhua Li,  ‡ Liyuan Zhou, ‡ Qian Zhang, Miao Yu and Xinhua Xiao  \*

Genistein has beneficial effects on glucose metabolism and adipose tissue browning which paralleled with gut microbiota alterations. However, the causality is unclear. This study aims to evaluate whether genistein could ameliorate metabolism and activate the browning program and whether gut microbiota is indispensable for these alterations. We examined the effect of 10-week genistein gavage (30 mg kg<sup>-1</sup> d<sup>-1</sup>) on glucose metabolism in C57BL/6J mice. Cecal contents were collected for 16s rRNA sequencing. The mRNA of browning markers was quantified in adipose tissues. Antibiotic administration was used to deplete gut microbiota. The lean mice with a normal control diet and genistein exhibited better glucose tolerance and higher expression of *UCP1* and *PGC1α* in white fat compared with those without genistein. Markedly enriched *Blautia*, *Ruminiclostridium\_5*, and *Ruminiclostridium\_9* in genistein-treated mice were significantly correlated with browning markers and glucose tolerance. In obese mice, genistein alleviated the detrimental effects of a high-fat diet on glucose homeostasis and increased *UCP1* and *PGC1α* expression in brown fat. Obvious increases in *Ruminiclostridium*, *Rikenella*, and *Clostridium\_sensu\_stricto\_1* by genistein were associated with metabolic improvement. However, depleting gut microbiota abolished these benefits. Overall, our findings indicated that gut microbiota contributed to enhanced glucose metabolism and adipose tissue browning of genistein, providing a promising target for metabolic health protection.

Received 9th July 2022,  
Accepted 30th September 2022

DOI: 10.1039/d2fo01973f

[rsc.li/food-function](https://rsc.li/food-function)

## Introduction

According to the latest data from the International Diabetes Federation (IDF), there were approximately 537 million adults with diabetes mellitus (DM) worldwide in 2021. If this growing trend continues, this number is expected to increase to 783 million in 2045.<sup>1</sup> The worldwide epidemic DM has resulted in tremendous economic and social burden. Type 2 diabetes mellitus (T2DM) accounts for more than 90% of global DM cases.<sup>2–4</sup> Obesity has been widely recognized in the pathogenesis of T2DM and considered to be an independent risk factor for it. Therefore, it is essential to find more effective strategies to inhibit and slow the occurrence and development of T2DM and obesity.

Taking advantage of their diverse biological activities and low toxicity, naturally occurring substances have been considered to be valuable resources for the development of new therapeutic agents in chronic metabolic disease treatment.<sup>5</sup>

Genistein is an isoflavone mainly found in soy products. The estimated intake of isoflavones in Asian populations consuming diets high in soy-based products is approximately 20–80 mg day<sup>-1</sup>.<sup>6–9</sup> While the typical Western diet contains far lower levels of genistein, followers of strict vegetarian diets would be expected to have intake levels approaching that of the Asian diet. Genistein has been investigated for protective effects in cognitive function,<sup>10</sup> cancer therapy,<sup>11</sup> and cardiovascular<sup>12</sup> and metabolic health.<sup>13,14</sup> The structural similarities between genistein and estradiol can partially elucidate the potential therapeutic and preventive actions of genistein exerted on diseases.<sup>15</sup> Concretely, genistein displays a broad range of effects on inflammation and NAD<sup>+</sup> metabolism.<sup>16</sup> It also induces insulin sensitivity, fatty acid metabolism, and adipocyte differentiation, and consequently improves glucose and lipid metabolism.<sup>13,17,18</sup> The identified potential pathways include improving oxidative stress,<sup>19–22</sup> inhibiting tyrosine kinase activities,<sup>23</sup> and enhancing *GLUT4* (glucose transporter type 4) and *PPARγ* (peroxisome proliferator-activated receptor gamma) expression.<sup>24</sup> Unfortunately, the exact mechanisms are not completely understood.

With the rapid development of high-throughput sequencing technology in microbiology, the gut microbiome has received increasing attention and is regarded as “forgotten metabolic organs”. Numerous recent studies have indicated that

Key Laboratory of Endocrinology, Ministry of Health, Department of Endocrinology, Peking Union Medical College Hospital, Peking Union Medical College, Chinese Academy of Medical Sciences, Beijing, China. E-mail: [xiaoxh2014@vip.163.com](mailto:xiaoxh2014@vip.163.com)

† Electronic supplementary information (ESI) available. See DOI: <https://doi.org/10.1039/d2fo01973f>

‡ These authors contributed equally to this work.



microbial dysbiosis was intertwined with metabolic perturbations. The evidence from human and animal studies has proved that there were significant differences in the gut microbiota of individuals with metabolic disorders (including glucose intolerance, insulin resistance and hyperlipidemia) and healthy individuals.<sup>25–28</sup> Limited studies and our previous research have reported that genistein intake significantly relieved glucose intolerance induced by a high-fat diet or attenuated the harmful effects of maternal overnutrition on metabolism in offspring accompanied by the modification of the gut microbiota.<sup>29–32</sup> However, little information is known about the causal relationship and molecular links between gut microbiota and the metabolic protection of genistein administration.

It is worth noting that genistein has been proposed as a promising “browning agent” to increase the expression of browning markers in white adipose tissue (WAT) and to stimulate the activation of brown adipose tissue (BAT).<sup>33–36</sup> Furthermore, accumulating data showed that gut microbiota is a vital endogenous factor in regulating white-to-brown fat conversion and non-shivering thermogenesis in BAT.<sup>37,38</sup> These results provide insight into the gut microbiota–adipose tissue signaling axis and beige fat development in the process of rehabilitation of metabolic dysfunction by genistein. Hence, we hypothesized that exposure to genistein could modulate glucose metabolism and the browning program of adipose tissues in mice. In addition, the present study depleted gut microbiota by a cocktail of antibiotics (ABX) to confirm its necessity in the role of genistein in promoting metabolic health.

## Materials and methods

### Animal model and experimental protocol

Four-week-old C57BL/6J female mice were purchased from Beijing HFK Bioscience Co., Ltd (Beijing, China, SCXK-2016-0006). Mice were housed in a specific pathogen-free (SPF) environment (room temperature of 20–24 °C and 12 h light/dark cycle) with *ad libitum* access to food and sterile water. For the lean mice fed a normal control diet (AIN-93G, 15.8% of the calories as fat), fifteen-week-old females were randomly assigned into three groups: (1) CD ( $n = 5$ ): treated by daily gavage with a vehicle (saline solution containing 3% DMSO, Sigma, Shanghai, China); (2) CG ( $n = 6$ ): administered genistein (30 mg kg<sup>−1</sup> day<sup>−1</sup>, freshly prepared in 3% DMSO solution) (CAS: 466-72-0, G0272, TCI Development Co., Ltd); and (3) CABX ( $n = 5$ ): treated with genistein accompanied by an antibiotic cocktail (ABX) drink (0.5 g L<sup>−1</sup> vancomycin, 1 g L<sup>−1</sup> metronidazole, 1 g L<sup>−1</sup> neomycin sulfate, and 1 g L<sup>−1</sup> ampicillin). Based on a series of safety studies with genistein,<sup>29,39,40</sup> the administration dosage in this study represented a level within the dose range that has been shown to elicit effects in laboratory animals. The dose translation from mice to human dose equivalents was calculated through normalization to the body surface area and using the formula shown in the ESI

Fig. 1.<sup>†</sup><sup>41</sup> This calculation results in a human equivalent dose for genistein of 2.4 mg kg<sup>−1</sup>, which is close to the daily consumption of soy products in Asian populations. While it may not be achievable through the typical Western diet, this concentration may be provided through a daily oral supplement.

To further explore the efficacy of genistein under an abnormal metabolic state, another high-fat diet induced obesity mouse model was established. Similarly, mice were fed with a high-fat diet starting at 5 weeks old for 10 weeks, and then were randomly divided into three groups: (1) HFD ( $n = 5$ ): high-fat diet fed mice with a vehicle; (2) HFG ( $n = 6$ ): high-fat diet fed mice with genistein; and (3) HFABX ( $n = 5$ ): high-fat diet fed mice with genistein and ABX.

The intervention of genistein and ABX lasted for 10 weeks. Body weight and food and water intake were measured every week. At the end of the experiment, all mice were sacrificed. Blood samples were collected from the intraorbital retrobulbar plexus after 10–12 h of fasting from anesthetized mice. The inguinal subcutaneous adipose tissue (SAT), perirenal visceral adipose tissue (VAT) and interscapular brown adipose tissue (BAT) were removed and weighed. The cecal contents were quickly removed, snap frozen in dry ice, and then stored at −80 °C for further analysis. The experimental design is shown in Fig. 1A and 4A. All work involving animals was performed according to the procedures approved by the Animal Care and Ethics Committee at Peking Union Medical College Hospital (Beijing, China, XHDW-2019012). All the animal operations were conducted in compliance with the National Institutes of Health guide for the care and use of laboratory animals.

### Intraperitoneal glucose tolerance tests (IPGTTs)

IPGTTs were performed three times, first before the start of genistein and ABX intervention (baseline), second at 5 weeks after genistein and ABX intervention, and third at the end of the experiment. After 6 h of fasting, glucose was injected intraperitoneally at 2 g per kg body weight. Blood glucose (BG) was measured in the blood from tail veins before injection (time 0 min) and 15, 30, 60, 90 and 120 min after glucose injection, using a Contour TS glucometer (Bayer, Beijing, China). The area under the curve (AUC) was calculated as previously described.<sup>42</sup>

### Serum biochemical parameter measurement

The blood samples collected at the end of the experiment were centrifuged at 3000g for 10 min at 4 °C, and the serum was stored in aliquots at −80 °C. Plasma glucose, free fatty acids (FFAs), total triglyceride (TG), total cholesterol (TC), high-density lipoprotein cholesterol (HDL-C), and low-density lipoprotein cholesterol (LDL-C) were measured using an autoanalyzer in the Peking Union Medical College Hospital. Plasma insulin was detected using the enzyme-linked immunosorbent assay (ELISA) kit (80-INSMSU-E01, Salem, NH, USA) according to the protocol provided by the supplier. Insulin sensitivity was assessed by homeostasis model assessment of insulin resistance (HOMA-IR), which was calculated as previously described.<sup>42</sup>



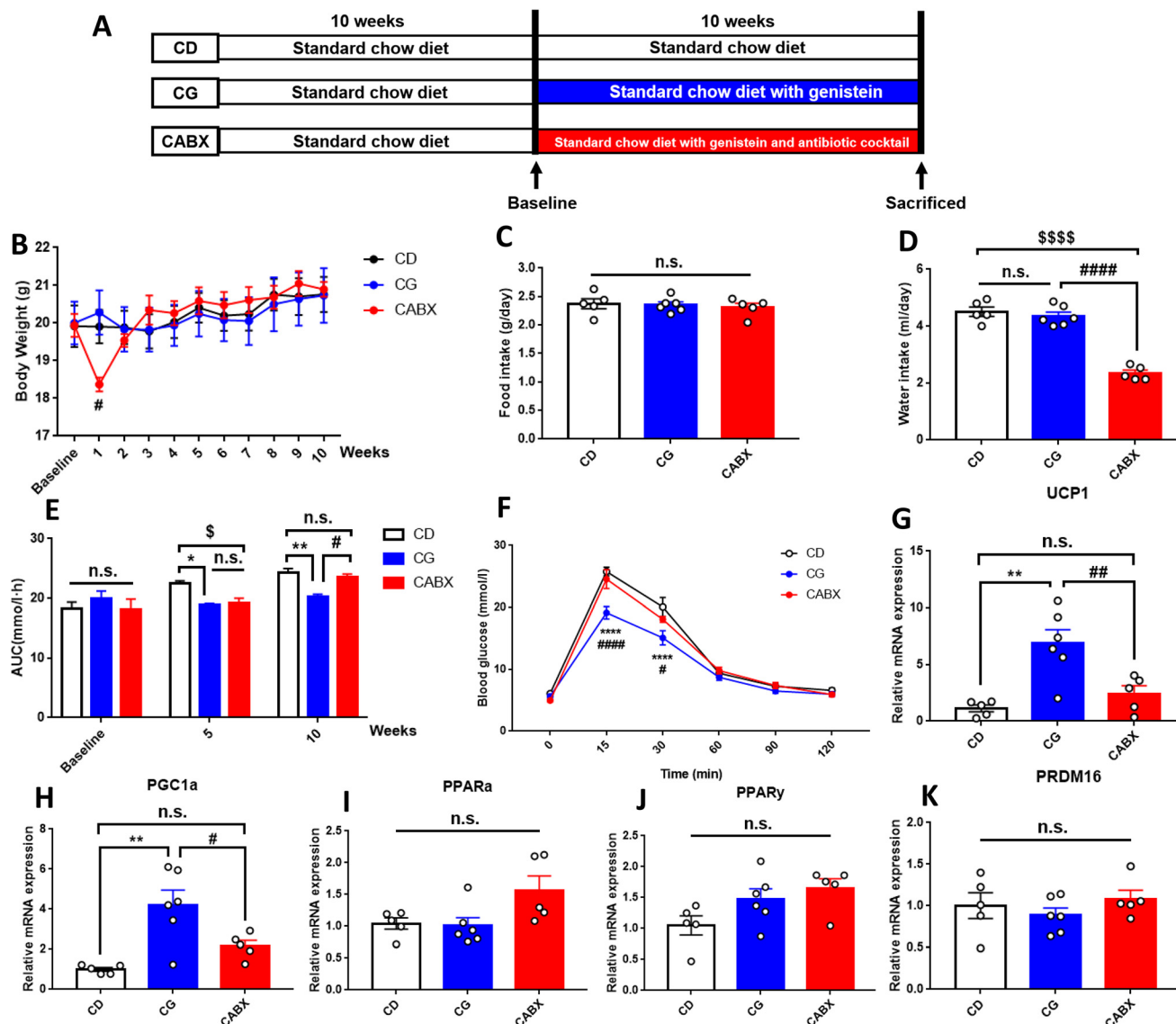


**Fig. 1** Genistein improved the glucose tolerance and enhanced the relative gene expression levels of browning markers in the inguinal subcutaneous adipose tissue of lean mice. (A) Experimental scheme; (B) the changes of body weight during the intervention period; (C) mean food intake during the experimental period expressed as grams per day; (D) mean water intake expressed as milliliters per day; (E) AUC of blood glucose values during intraperitoneal glucose tolerance tests; (F) intraperitoneal glucose tolerance test at the end of experiment; (G) relative gene expression levels of *UCP1*; (H) relative gene expression levels of *PGC1α*; (I) relative gene expression levels of *PPARα*; (J) relative gene expression levels of *PPARγ*; (K) relative gene expression levels of *PRDM16*. CD, normal control diet with a vehicle; CG, normal control diet with genistein; CABX, normal control diet with genistein and antibiotic cocktail. AUC, area under the curve; *UCP1*, uncoupling protein 1; *PGC1α*, peroxisome proliferator-activated receptor gamma coactivator 1-alpha; *PPARα*, peroxisome proliferator-activated receptor alpha; *PPARγ*, peroxisome proliferator-activated receptor gamma; *PRDM16*, positive regulatory domain containing 16. Data are expressed as means  $\pm$  S.E.M. ( $n = 5-6$  per group) and were analyzed by one-way ANOVA or two-way ANOVA, with Turkey *post hoc* analyses. Mean values were significantly different between the groups: \* $p < 0.05$ , \*\* $p < 0.01$ , \*\*\* $p < 0.0001$ ; #CG vs. CABX, # $p < 0.05$ , ### $p < 0.01$ , ##### $p < 0.0001$ ; \$CABX vs. CD, \$ $p < 0.05$ , \$\$\$\$ $p < 0.0001$ .

### Gut microbiota analysis

Microbial DNA was extracted from the cecal contents using a DNA isolation kit (MN NucleoSpin 96 Soi, MACHEREY-NAGEL, Dueren, Germany) according to the manufacturer's protocols. The V3–V4 regions of the 16S rRNA genes were amplified with the common primer pair (338F, 5'-ACTCCTACGGGA-GGCAGCA-3'; 806R, 5'-GGACTACHVGGGTWCTAAT-3'), which

included barcode sequences and adapters. Amplicons were purified using the OMEGA Cycle Pure kit (D6492-02, Omega Bio-Tek, USA) and Monarch DNA gel extraction kit (T1020L, New England BioLabs, MA, USA). The tags were sequenced on the Illumina HiSeq 2500 PE250 platform (Illumina, Inc., CA, USA).

A total of 2 560 330 reads was generated and then merged using the FLASH software<sup>43</sup> (version 1.2.11). After merging

paired-end reads, reads were performed by quality filtering (Trimmomatic,<sup>44</sup> version 0.33) and chimera detection (UCHIME,<sup>45</sup> version 8.1). High quality reads were clustered into operational taxonomic units (OTUs) with 97% similarity using the UPARSE software<sup>46</sup> (version 10.0), and representative sequences for each OTU were screened using the QIIME2 software<sup>47</sup> (version 2020.6, Center for Microbiome Innovation, University of California San Diego, La Jolla, CA, USA). Then, the RDP Classifier<sup>48</sup> (version 2.2) was used to annotate taxonomic information. Alpha and beta diversity analyses were achieved using the QIIME2 and R software (Version 3.1.1). For alpha diversity, Chao1, Ace, Shannon and Simpson indexes were analyzed. For beta diversity, principal coordinate analysis (PCoA) plots and analysis of similarities (ANOSIM) were performed using the Bray–Curtis measure. Additionally, linear discriminant analysis (LDA) of the effect size (LEfSe) was used to determine differences among the groups. The datasets presented in this study can be found in online repositories.

### qRT-PCR experiments

Total RNA from frozen BAT and WAT was extracted *via* the RNA-Solv® reagent (Omega Bio-Tek Inc., Guangzhou, China) according to the manufacturer's instructions. The quality and concentration of RNA were analyzed on Nanodrop (ND-1000; NanoDrop Products, Wilmington, DE, USA). 1 µg of total RNA was used as the template for cDNA synthesis using the PrimeScript™ RT reagent kit with gDNA Eraser (RR047A, TaKaRa Bio Inc., Otsu, Shiga, Japan). Real-time PCR was performed using TB Green PCR Master Mix (RR820A, Takara Bio Inc., Otsu, Shiga, Japan) and quantitative PCR was carried out in triplicate using a 96 well PCR microplate for ABI 7500 thermocycler (Applied Biosystems, CA, USA) in a 20 µL reaction volume. The reaction conditions consisted of an initial activation step (30 s at 95 °C) and a cycling step (denaturation for 5 s at 95 °C and annealing for 34 s at 60 °C for 40 cycles). The following six genes related to WAT browning or BAT thermogenesis were evaluated: *UCP1* (uncoupling protein 1), *PGC1α* (peroxisome proliferator-activated receptor gamma coactivator

1-α), *PPARα* (peroxisome proliferator-activated receptor alpha), *PPARγ* (peroxisome proliferator-activated receptor gamma) and *PRDM16* (positive regulatory domain containing 16). The relative expression levels of each gene were normalized to *PPIA* (peptidylprolyl isomerase A). The specificity of the amplified genes was verified by dissociation curves. The primer sequences used in this study are provided in the ESI Table 1.† RNA expression data were analyzed according to the  $2^{-\Delta\Delta Ct}$  method.

### Statistical analysis

Statistical analyses were completed using Prism version 7.0 (GraphPad Software Inc., San Diego, CA, USA) with  $p < 0.05$  used to determine statistical significance of all comparisons. Data are presented as the means ± standard error of the means (S.E.M.). Multiple comparisons between groups were performed by one-way ANOVA and two-way ANOVA, with Tukey's and Bonferroni *post hoc* analyses. The relationships between the relative abundance of bacterial taxa at the genus level and browning markers as well as IPGTT AUC were analysed by Spearman's correlation analysis.

## Results

### The effects of genistein and antibiotic cocktail administration on metabolic phenotype in lean mice

During the 10-week genistein intervention, there was no significant difference between the CD and the CG groups in body weight, adipose tissue content, average food or water intake (Fig. 1B–D and Table 1). However, compared with the genistein diet fed without ABX drink mice, the body weight of the ABX-treated mice decreased dramatically within 1 week and returned to the original weight in the second week. Besides, the CABX group exhibited a striking decline in water intake.

An IPGTT was performed to explore the effect of genistein on glucose metabolism of mice. At the end of the treatment, we observed that genistein attenuated the elevation of blood

**Table 1** Adipose tissue mass and metabolic parameters of lean mice

Parameters	CD ( $n = 5$ )	CG ( $n = 6$ )	CABX ( $n = 5$ )
SAT (g)	0.134 ± 0.023	0.132 ± 0.018	0.118 ± 0.001
VAT(g)	0.098 ± 0.036	0.113 ± 0.034	0.052 ± 0.021
BAT (g)	0.112 ± 0.012	0.095 ± 0.011	0.090 ± 0.007
TC (mmol l <sup>-1</sup> )	2.476 ± 0.049	2.506 ± 0.079	3.060 ± 0.249 <sup>#</sup>
TG (mmol l <sup>-1</sup> )	0.149 ± 0.044	0.096 ± 0.011	0.138 ± 0.032
LDL-C (mmol l <sup>-1</sup> )	0.194 ± 0.011	0.214 ± 0.005	0.383 ± 0.048 <sup>#</sup>
HDL-C (mmol l <sup>-1</sup> )	1.047 ± 0.017	1.062 ± 0.049	1.252 ± 0.059 <sup>#</sup>
FFA (µmol l <sup>-1</sup> )	975.800 ± 95.980	1004.000 ± 29.910	1039.000 ± 50.170
Insulin (ng ml <sup>-1</sup> )	0.157 ± 0.030	0.194 ± 0.026	0.147 ± 0.011
HOMA-IR	1.003 ± 0.253	1.239 ± 0.189	0.820 ± 0.108

CD, normal control diet with a vehicle; CG, normal control diet with genistein; CABX, normal control diet with genistein and antibiotic cocktail. SAT, subcutaneous adipose tissue; VAT, visceral adipose tissue; BAT, brown adipose tissue; TC, total cholesterol; TG, triacylglycerol; HDL-C, high density lipoprotein cholesterol; LDL-C, low-density lipoprotein cholesterol; FFA, free fatty acid; and HOMA-IR, homeostasis model assessment of insulin resistance. Data are expressed as means ± S.E.M. ( $n = 5$ –6 per group). Mean values were significantly different between the groups: \*CABX vs. CD,  $p < 0.05$ ; <sup>#</sup>CABX vs. CG,  $p < 0.05$ .



glucose at 15 min ( $p < 0.0001$ ) and 30 min ( $p < 0.0001$ ) as well as reduced the AUC ( $p < 0.01$ ) in comparison with those in the CD group (Fig. 1E and F). Conversely, gut microbiota depletion counteracted these benefits. In addition to glucose tolerance, insulin sensitivity of mice was also evaluated. As shown in

Table 1, genistein did not exert effects on fasting insulin levels or HOMA-IR index.

To explore the effects of genistein on lipid metabolism, we measured the serum levels of TC, TG, HDL-C, LDL-C, and FFAs. Unfortunately, no significant difference was found

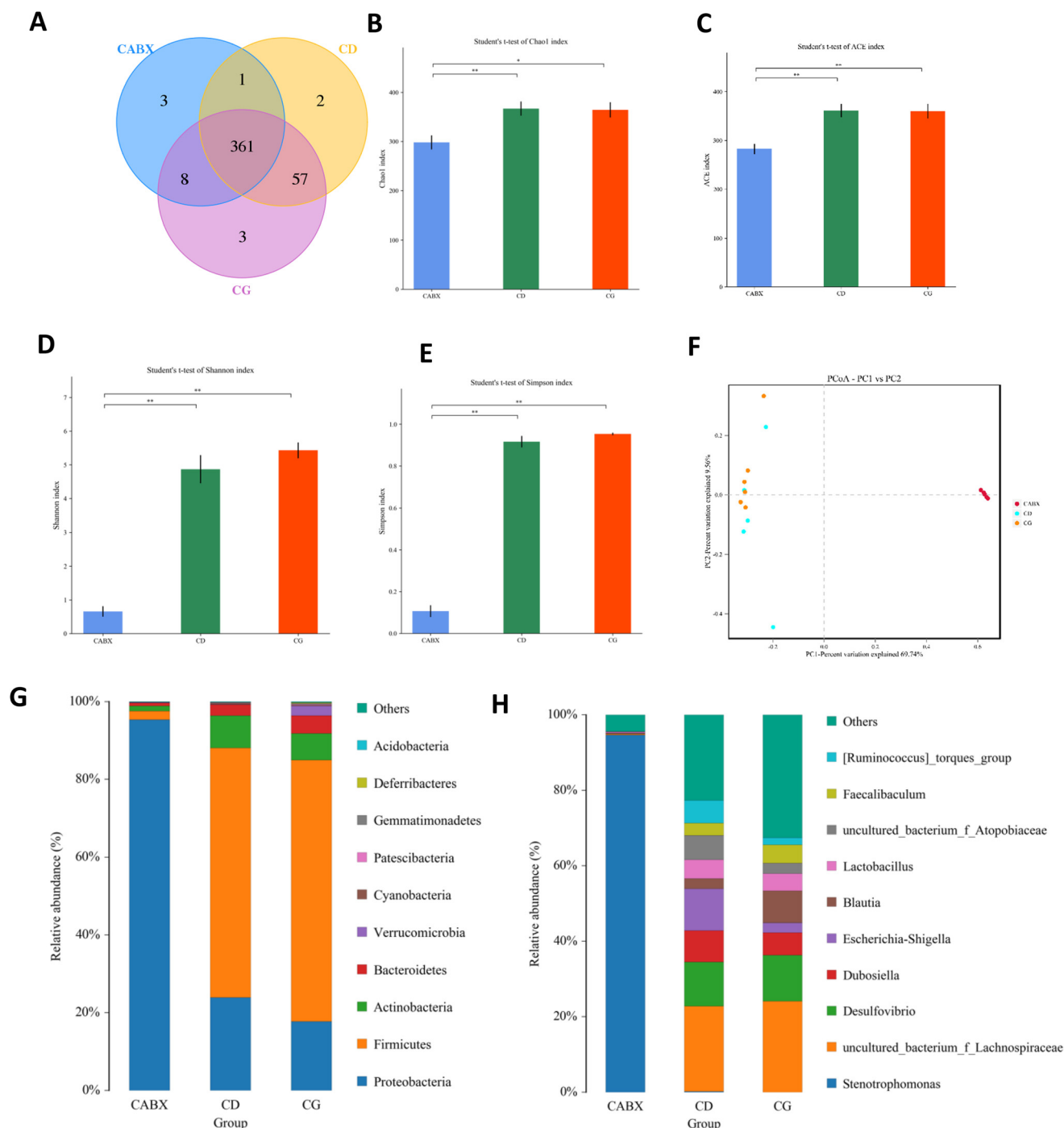


**Fig. 2** Genistein altered the gut microbiota in lean mice. (A) Venn diagram of the OTUs; (B) Chao index; (C) ACE index; (D) Simpson index; (E) Shannon index; (F) PCoA plots of gut microbiome; (G) relative abundance of the top 10 phyla; (H) relative abundance of the top 10 genera; (I) the LEfSe analysis of the different gut microbiota from the phylum level down to the genus level. CD, normal control diet with a vehicle; CG, normal control diet with genistein; CABX, normal control diet with genistein and antibiotic cocktail. Data are expressed as means  $\pm$  S.E.M. ( $n = 5-6$  per group). Differences with  $P < 0.05$  were considered to be significant. \* $p < 0.05$ , \*\* $p < 0.01$ .





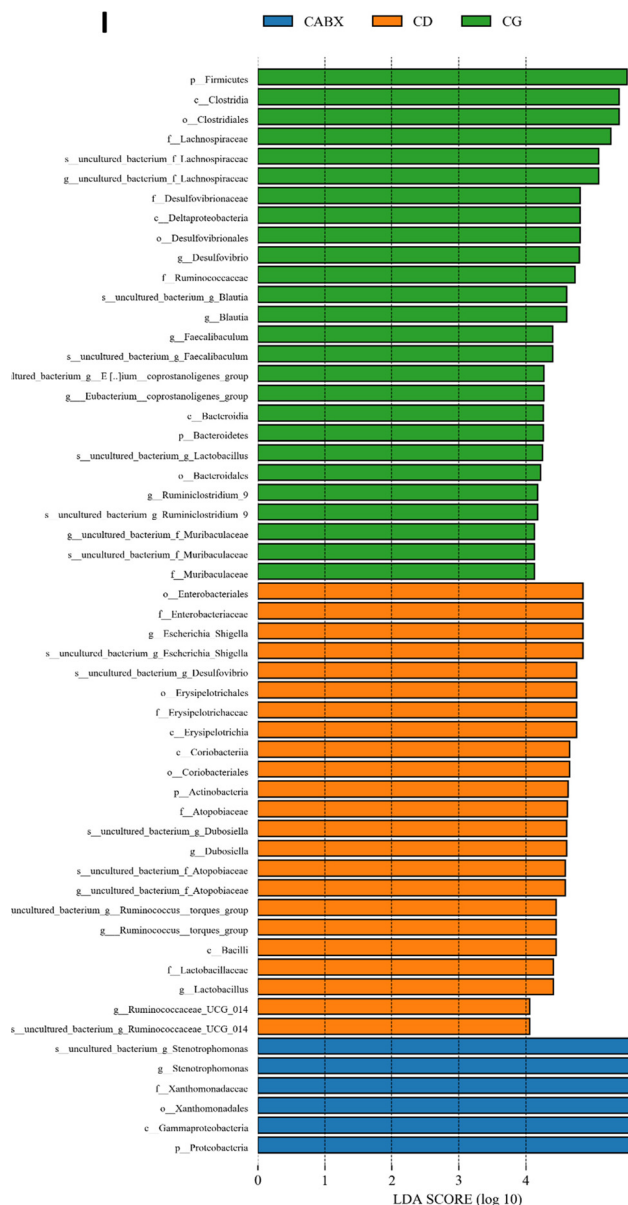


Fig. 2 (Contd.).

between CD and CG groups, but the serum TC ( $p < 0.05$ ), LDL-C ( $p < 0.05$ ), and HDL-C ( $p < 0.05$ ) levels were significantly higher in mice from the CABX group than those from other two groups (Table 1).

### Genistein-treated lean mice exhibited white adipose tissue browning

There is evidence that the improvement in carbohydrate metabolism is associated with metabolic changes occurring in the adipose tissue.<sup>49,50</sup> In response to stimulation, brown fat cells also emerge in the WAT (named beige cells) through the expression of BAT typical markers, a process known as browning. In this study, the expression pattern associated with WAT browning was detected in the mice that were administered

genistein. The increases in the *UCP1* and *PGC1 $\alpha$*  expression were approximately 7- and 4-fold, respectively (Fig. 1G and H). It is noteworthy that ABX administration reversed the expression of the above genes back to the same level as in the CD group, suggesting that the lack of gut microbiota could interfere with the genistein-induced WAT browning. However, the expression of brown fat specific markers in the interscapular BAT did not significantly differ among these three groups (ESI Fig. 2<sup>†</sup>).

### Gut microbiota contributes to the beneficial effects of genistein on glucose homeostasis in lean mice

16s rRNA gene sequencing was applied to verify the causality of gut microbiota modification and the enhanced glucose metabolism induced by genistein intervention. The Venn diagram showed that there were 361 shared OTUs among the three groups, 2 unique OTUs in the control diet fed mice, 3 OTUs in the CG group and 3 unique OTUs in the mice treated with genistein and ABX (Fig. 2A). The results of alpha diversity showed that microbial diversity and richness had no difference between CD and CG groups, but remarkably decreased in the CABX group (Fig. 2B–E). As shown in Fig. 2F, PCoA revealed that the intestinal microbiota was separated among the three groups, which was further confirmed by ANOSIM ( $R^2 = 0.735$ ,  $p = 0.001$ ). The relative abundance of the top 10 phyla and genera are listed in Fig. 2G and H. At the phylum level, *Firmicutes*, *Bacteroidetes*, *Actinobacteria*, and *Proteobacteria* were the most abundant, whereas the relative abundance of the four phyla were not significantly different between the CD and CG groups. However, ABX exposure greatly altered the composition of the gut microbiota, and compared with other two groups, the dominant phyla shifted from *Firmicutes* and *Bacteroidetes* to *Proteobacteria* (Fig. 3A–C). At the genus level, genistein dramatically increased the relative abundance of *Ruminiclostridium\_5* ( $p < 0.05$ ), *Ruminiclostridium\_9* ( $p < 0.01$ ), and *Blautia* ( $p < 0.0001$ ), as well as a growth tendency in *Faecalibaculum* ( $P = 0.08$ ) when compared to the control group. In contrast, all of these genera were markedly retrogressed by ABX treatment ( $p < 0.01$  and  $p < 0.0001$ ) (Fig. 3D–G). We further dissected the individual microbial species differentially enriched among the three groups from the phylum level to the genus level. The result of LefSe analysis was consistent with the above findings (Fig. 2I).

### Correlation analyses between gut microbiota and browning markers in WAT as well as glucose tolerance in lean mice

Next, to explore the relationship between the abundance of significantly altered bacteria at the genus level and WAT browning as well as glucose tolerance, we did the Spearman correlation analysis. The results indicated that significantly enriched genera *Blautia*, *Ruminiclostridium\_5* and *Ruminiclostridium\_9* by genistein administration were all positively correlated with the relative expression of browning markers (*UCP1* and *PGC1 $\alpha$* ) and negatively related with the AUC of IPGTTs (Fig. 3H).



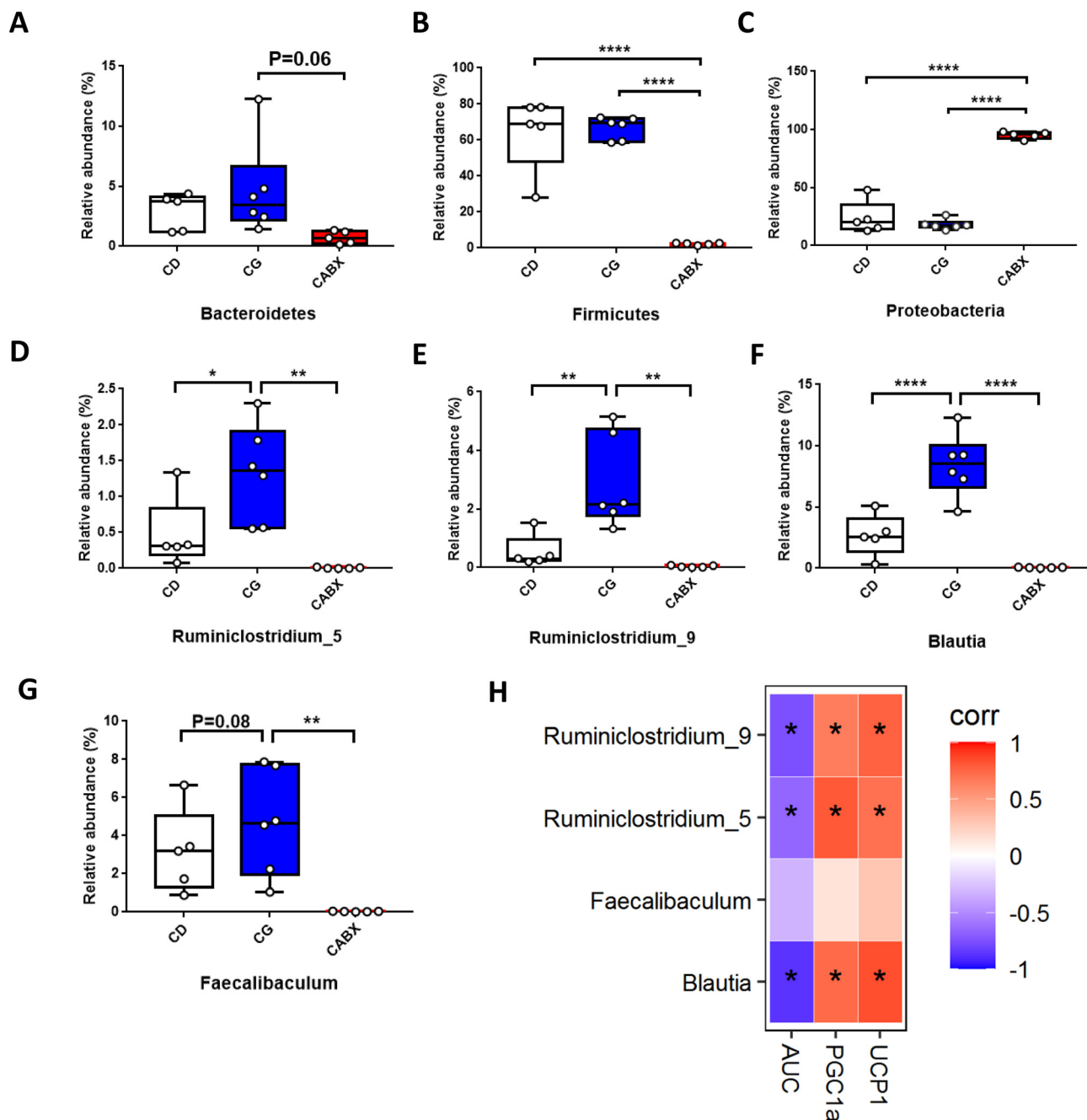


**Fig. 3** Relative abundance of bacterial taxa at different taxonomic levels and the correlation analysis between these dramatically altered genera and the relative expression of browning markers in WAT as well as glucose tolerance in lean mice. (A) Phylum *Bacteroidetes*; (B) phylum *Firmicutes*; (C) phylum *Proteobacteria*; (D) genus *Ruminiclostridium\_5*; (E) genus *Ruminiclostridium\_9*; (F) genus *Blautia*; (G) genus *Faecalibaculum*; (H) heatmap of spearman correlation analysis. CD, normal control diet with a vehicle; CG, normal control diet with genistein; CABX, normal control diet with genistein and antibiotic cocktail. AUC, area under the curve of IPGTTs; *UCP1*, uncoupling protein 1; *PGC1α*, peroxisome proliferator-activated receptor gamma coactivator 1- $\alpha$ . The statistics were analyzed by MetaStat or spearman correlation analysis ( $n = 5-6$  per group). Differences with  $P < 0.05$  were considered to be significant. \* $p < 0.05$ , \*\* $p < 0.01$ , \*\*\*\* $p < 0.0001$ .

### Genistein administration ameliorates high fat diet-driven glucose metabolic disorder

To further explore the effect of genistein in improving metabolic dysfunction, an investigation was conducted on obesity

mice induced by a high-fat diet. In line with lean mice, 10-week genistein therapy did not significantly change the body weight, adipose tissue content, average food or water intake of mice fed a high-fat diet (Fig. 4B–D). In order to determine whether genistein gavage could fight against the deleter-



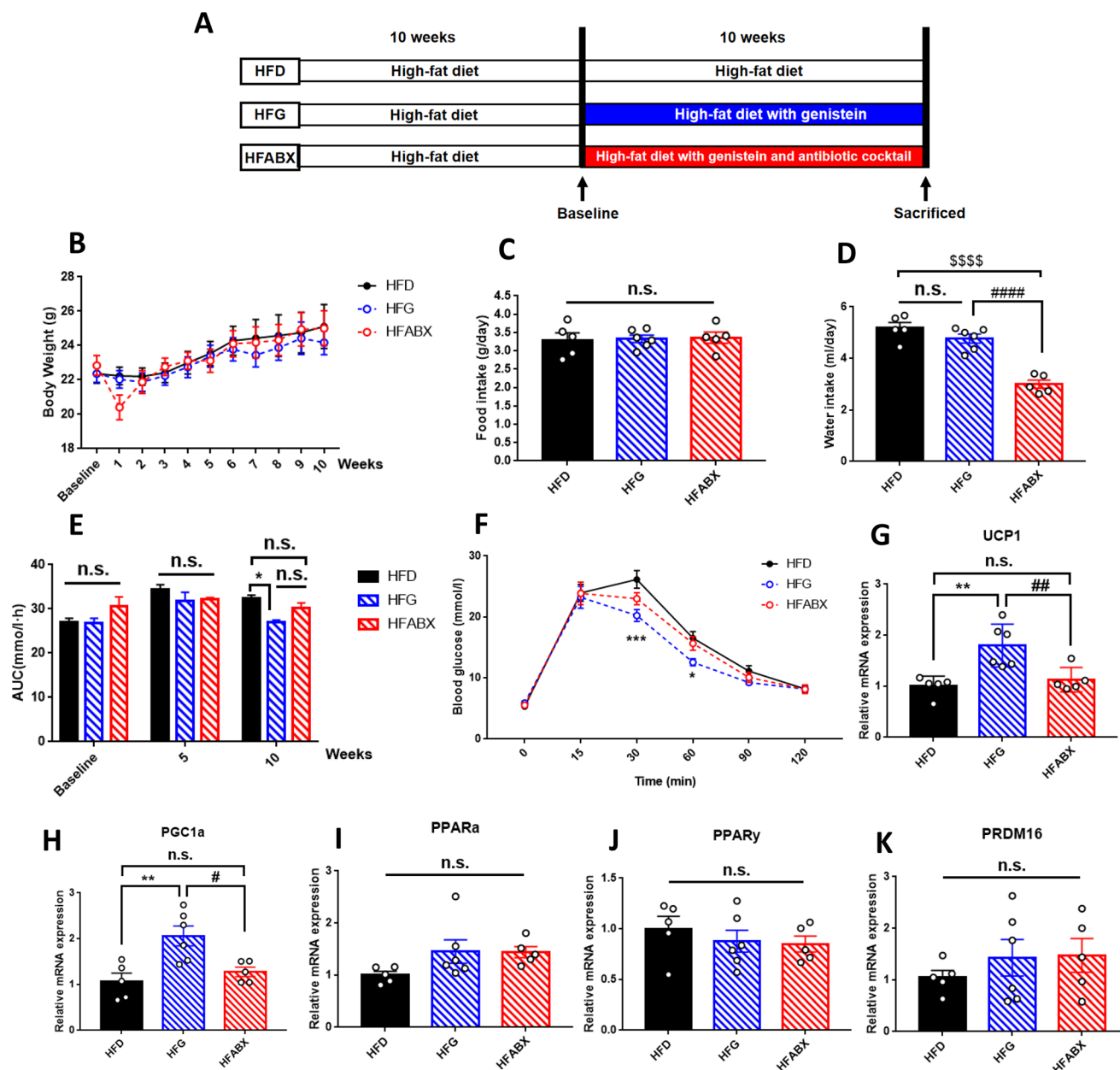


**Fig. 4** Genistein improved the glucose tolerance and enhanced the relative gene expression levels of thermogenesis indicators in the interscapular brown adipose tissue of obesity mice. (A) Experimental scheme; (B) the changes of body weight during the intervention period; (C) mean food intake during the experimental period expressed as grams per day; (D) mean water intake expressed as milliliters per day; (E) AUC of blood glucose values during intraperitoneal glucose tolerance tests; (F) intraperitoneal glucose tolerance test at the end of experiment; (G) relative gene expression levels of *UCP1*; (H) relative gene expression levels of *PGC1α*; (I) relative gene expression levels of *PPARα*; (J) relative gene expression levels of *PPARγ*; (K) relative gene expression levels of *PRDM16*. HFD, high-fat diet with a vehicle; HFG, high-fat diet with genistein; HFABX, high-fat diet with genistein and antibiotic cocktail. AUC, area under the curve; *UCP1*, uncoupling protein 1; *PGC1α*, peroxisome proliferator-activated receptor gamma coactivator 1- $\alpha$ ; *PPARα*, peroxisome proliferator-activated receptor alpha; *PPARγ*, peroxisome proliferator-activated receptor gamma; *PRDM16*, positive regulatory domain containing 16. Data are expressed as means  $\pm$  S.E.M. ( $n = 5-6$  per group) and were analyzed by one-way ANOVA or two-way ANOVA, with Turkey *post hoc* analyses. Mean values were significantly different between the groups: \*HFG vs. HFD, \* $p < 0.05$ , \*\* $p < 0.01$ , \*\*\* $p < 0.0001$ ; #HFG vs. HFABX, # $p < 0.05$ , ## $p < 0.01$ , #### $p < 0.0001$ ;  $^{\S}$ HFABX vs. HFD,  $^{\S\S\S\S}$  $p < 0.0001$ .

ious effects of high-fat diet on glucose tolerance, we performed IPGTTs for the three groups. As shown in Fig. 4E and F, obesity mice from the HFG group demonstrated a marked improvement in glucose tolerance. The blood glucose levels at

30 min ( $p < 0.001$ ), 60 min ( $p < 0.05$ ) and AUC ( $p < 0.05$ ) were significantly lower than in the HFD and HFABX groups. Meanwhile, we measured the fasting serum insulin levels and calculated the HOMA-IR index to investigate the effects of gen-





**Table 2** Adipose tissue mass and metabolic parameters of obesity mice

Parameters	HFD ( <i>n</i> = 5)	HFG ( <i>n</i> = 6)	HFABX ( <i>n</i> = 5)
SAT (g)	0.338 ± 0.081	0.338 ± 0.015	0.310 ± 0.090
VAT(g)	0.0180 ± 0.038	0.148 ± 0.027	0.130 ± 0.043
BAT (g)	0.126 ± 0.021	0.107 ± 0.017	0.098 ± 0.016
TC (mmol l <sup>-1</sup> )	3.184 ± 0.337	3.089 ± 0.240	2.912 ± 0.160
TG (mmol l <sup>-1</sup> )	0.141 ± 0.031	0.107 ± 0.016	0.192 ± 0.028
LDL-C (mmol l <sup>-1</sup> )	0.236 ± 0.036	0.209 ± 0.027	0.216 ± 0.016
HDL-C (mmol l <sup>-1</sup> )	1.243 ± 0.094	1.270 ± 0.092	1.303 ± 0.038
FFA (μmol l <sup>-1</sup> )	706.900 ± 61.450	726.700 ± 91.080	753.000 ± 59.09
Insulin (ng ml <sup>-1</sup> )	0.321 ± 0.058	0.189 ± 0.001*	0.161 ± 0.011 <sup>#</sup>
HOMA-IR	2.723 ± 0.319	1.517 ± 0.116**	1.297 ± 0.086 <sup>###</sup>

HFD, high-fat diet with a vehicle; HFG, high-fat diet with genistein; HFABX, high-fat diet with genistein and antibiotic cocktail. SAT, subcutaneous adipose tissue; VAT, visceral adipose tissue; BAT, brown adipose tissue; TC, total cholesterol; TG, triacylglycerol; HDL-C, high density lipoprotein cholesterol; LDL-C, low-density lipoprotein cholesterol; FFA, free fatty acid; and HOMA-IR, homeostasis model assessment of insulin resistance. Data are expressed as means ± S.E.M. (*n* = 5–6 per group). Mean values were significantly different between the groups: \*HFG vs. HFD, *p* < 0.05, \*\**p* < 0.01; <sup>#</sup>HFABX vs. HFD, *p* < 0.05, <sup>###</sup>*p* < 0.001.

istein intervention on insulin sensitivity under the state of metabolic disturbance. Significantly decreased insulin levels (*p* < 0.05) and smaller HOMA-IR index (*p* < 0.01) were observed in the HFG group compared with that in the HFD group. Although the differences in glucose metabolism were prominent, there were no differences in the serum lipid profiles among the three groups (Table 2).

#### Genistein enhances the activation of brown adipose tissue in obesity mice

To further clarify whether genistein could activate the browning program in adipose tissue and whether microbiota depletion could prevent this process in obese mice, we examined the expression of brown adipocyte-specific genes in SAT and BAT. Although we did not observe differential expression of WAT browning markers in SAT among the three groups (ESI Fig. 3†), the relative expression of *UCP1* and *PGC1α* were drastically increased in BAT of the HFG group compared with the other two groups (Fig. 4G–H). Thus, from these results, it was possible to assume that genistein was able to activate the thermogenic function of BAT, whereas gut microbiota depletion by ABX prevented it from exerting the metabolic protective effect.

#### Gut microbiota is required for genistein-induced glucose improvement in obesity mice

Given that gut microbiota mediated the protective effect of genistein on glucose metabolism in lean mice, we further assessed the influence of genistein supplementation on gut microbiota in mice fed a high-fat diet. 331 shared OTUs, 4 unique OTUs in the HFD-fed mice, 8 unique OTUs in the HFG-fed mice, and 3 unique OTUs in the HFG-fed mice combined with ABX administration are shown in the Venn diagram (Fig. 5A). Alpha diversity analysis showed that there were obvious differences in the community richness and diversity among the three groups. Specifically, the Simpson and Shannon indexes were significantly higher in the HFG group compared with the HFD group, while ABX exposure tremendously depleted commensal microflora (Fig. 5B–E). On the

basis of PCoA analysis, we found that genistein intervention induced distinct separation between the HFG and HFD groups, and the ABX-treated groups were quite distant from the other two groups (Fig. 5F). Besides, this result was supported by ANOSIM analysis (*R*<sup>2</sup> = 0.753, *p* = 0.001). Consistent with the composition of microbiota in lean mice, *Firmicutes*, *Bacteroidetes*, *Actinobacteria*, and *Proteobacteria* were also the most abundant species at the phylum level in obesity mice (Fig. 4G). In particular, the relative abundance of *Firmicutes* (*p* < 0.05) was significantly increased in mice after genistein supplementation compared with those in the HFD group. The shift from *Firmicutes* and *Bacteroidetes* to *Proteobacteria* was still noticed in the HFABX group (Fig. 6A–C). Top 10 genera are listed in Fig. 4H and markedly different species from the phylum level to the genus level among the three groups were concluded in Fig. 4I. In comparison with the HFD group, *Ruminiclostridium* (*p* < 0.05), *Rikenella* (*p* < 0.05), *Clostridium\_sensu\_stricto\_1* (*p* < 0.05), and *Roseburia* (*p* < 0.0001) were significantly enriched in the HFG group at the genus level. Notably, the relative abundance of these potential probiotics were eliminated by ABX treatment (Fig. 6D–G).

#### Correlation analyses between gut microbiota and thermogenesis indicators in BAT as well as glucose tolerance in obesity mice

Finally, to investigate the relationship between gut microbiota, BAT activation and glucose metabolism, we performed the correlation analysis between the relative abundance of altered germs at the genus level, the relative expression level of BAT thermogenesis indicators and the AUC of IPGTTs. As shown in Fig. 6H, the elevated expression of *PGC1α* in BAT was positively related to the significantly enriched genus *Ruminiclostridium* in the HFG group. The relative abundances of *Ruminiclostridium*, *Rikenella*, *Clostridium\_sensu\_stricto\_1* and *Roseburia*, which were elevated by 10 weeks of genistein gavage, were all positively correlated with upregulated *UCP1* expression of BAT and negatively correlated with the AUC of IPGTTs.



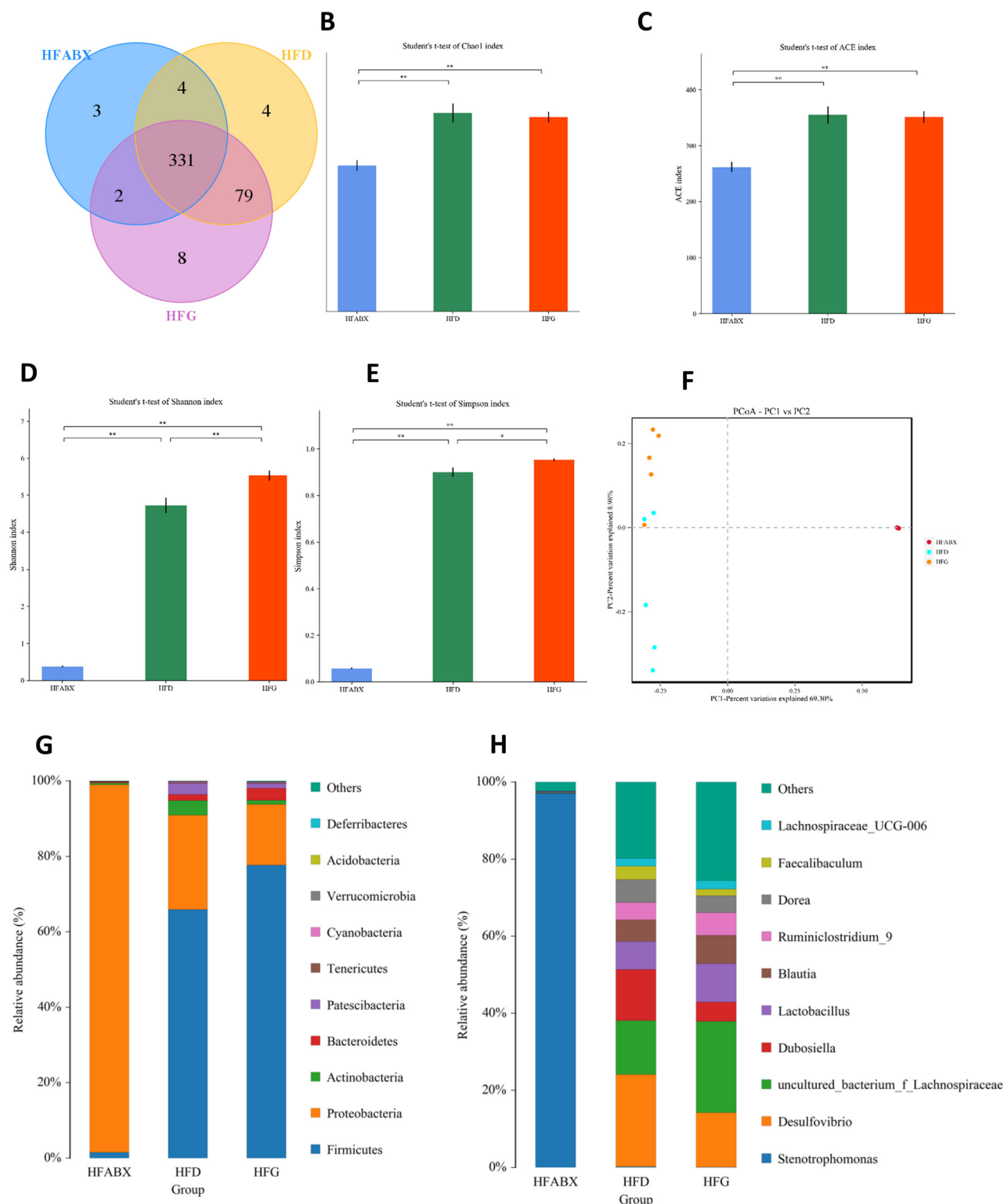


**Fig. 5** Genistein altered the gut microbiota in obesity mice. (A) Venn diagram of the OTUs; (B) Chao index; (C) ACE index; (D) Simpson index; (E) Shannon index; (F) PCoA plots of gut microbiome; (G) relative abundance of the top 10 phyla; (H) relative abundance of the top 10 genera; (I) the LEfSe analysis of the different gut microbiota from the phylum level down to the genus level. HFD, high-fat diet with a vehicle; HFG, high-fat diet with genistein; HFABX, high-fat diet with genistein and antibiotic cocktail. Data are expressed as means  $\pm$  S.E.M. ( $n = 5-6$  per group). Differences with  $P < 0.05$  were considered to be significant. \* $p < 0.05$ , \*\* $p < 0.01$ .



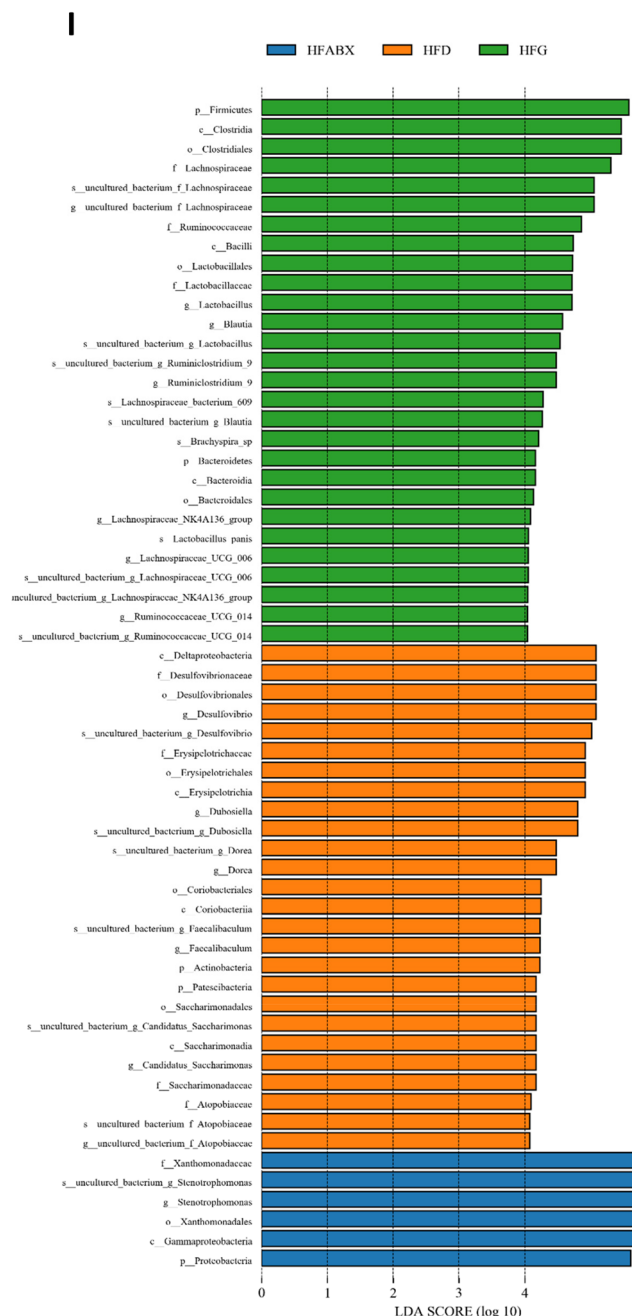


Fig. 5 (Contd.).

## Discussion

The prevalence of T2DM has been increasing dramatically worldwide, but current treatment strategies seem to be insufficient to halt the rapid progression of this epidemic. In recent years, bioactive dietary compounds have been developed into a topical issue in metabolism field. An increasing number of studies have suggested that genistein, a soy-derived bioactive isoflavone with estrogenic properties, has diverse favorable bioactivities, including anti-inflammatory, anti-diabetic, and hypolipidemic effects.<sup>13,14,16–18</sup> Our previous reports have

investigated that the alterations in the gut microbiota might contribute to the profits of genistein on glucolipid metabolic amelioration.<sup>30–32</sup> However, the causality between gut microbiota and the metabolic protective effect of genistein is unknown yet. In the current research, we discovered that genistein gavage significantly improved glucose metabolism and promoted adipose tissue browning in mice fed with a normal control diet or high-fat diet, whereas the benefit was abolished by ABX treatment. These findings illustrated that gut microbiota is essential for the beneficial effects of genistein on metabolic homeostasis.

Indeed, 16s rRNA sequencing revealed that the genus *Blautia*, genus *Ruminiclostridium\_5* and genus *Ruminiclostridium\_9* were markedly enriched in the cecal contents of the genistein intervention group compared with that in the normal control diet group. According to previous reports, *Blautia* species showed effective utilization of carbohydrates such as fiber and starch.<sup>51</sup> The main final products of glucose fermentation by *Blautia* is acetic acid, which may inhibit insulin signaling and fat accumulation in adipocytes through activating the G protein-coupled receptors *GPR41* and *GPR43*, thereby promoting the metabolism of unbound lipids and glucose in other tissues and thus maintaining glucose homeostasis and alleviating obesity-related diseases.<sup>52</sup> Corresponding to these characteristics, the abundance of *Blautia* was negatively related to visceral fat accumulation, body weight, the levels of fasting plasma glucose and hemoglobin A1C (HbA1c) in individuals with overweight/obesity or diabetes.<sup>53</sup> Moreover, another study found that berberine and metformin attenuated metabolic disturbance in high-fat diet-induced obesity rats, increasing the abundance of *Blautia*.<sup>54</sup> *Ruminiclostridium\_5* and *Ruminiclostridium\_9* are two members from the Ruminococcaceae family and were also implicated in the positive health states. More specifically, high-fat diet consumption in a rat model decreased the relative abundance of *Ruminiclostridium\_5*, whereas a prebiotic diet recovered it.<sup>55</sup> Song *et al.*<sup>56</sup> and Xiao *et al.*<sup>57</sup> respectively expounded that fruit extract (*Vaccinium bracteatum* Thunb.) and Chinese herbs (*Scutellariae Radix* and *Coptidis Rhizoma*) ameliorated glycolipid metabolism in obese mice and T2DM rats, accompanied by an increase in the number of *Ruminiclostridium\_9*. As short chain fatty acid (SCFA) producers, *Ruminiclostridium\_5* and *Ruminiclostridium\_9* were associated with the release of inflammatory and cytotoxic factors from the gut for maintenance of a stable intestinal microecology.<sup>58,59</sup> More interestingly, correlation analysis showed that these three bacterial genera were correlated with advanced glucose tolerance in the CG group compared to the CD group, whereas ABX administration counteracted these alterations. Thus, the genera *Blautia*, *Ruminiclostridium\_5* and *Ruminiclostridium\_9* might play crucial roles in the improved glucose metabolism by genistein.

When a high-fat diet, considered to be a metabolic stressor, was administered to mice, our results showed that the relative abundance of the genus *Ruminiclostridium*, genus *Rikenella*, genus *Clostridium\_sensu\_stricto\_1*, and genus *Roseburia* were significantly decreased, which were negatively correlated with



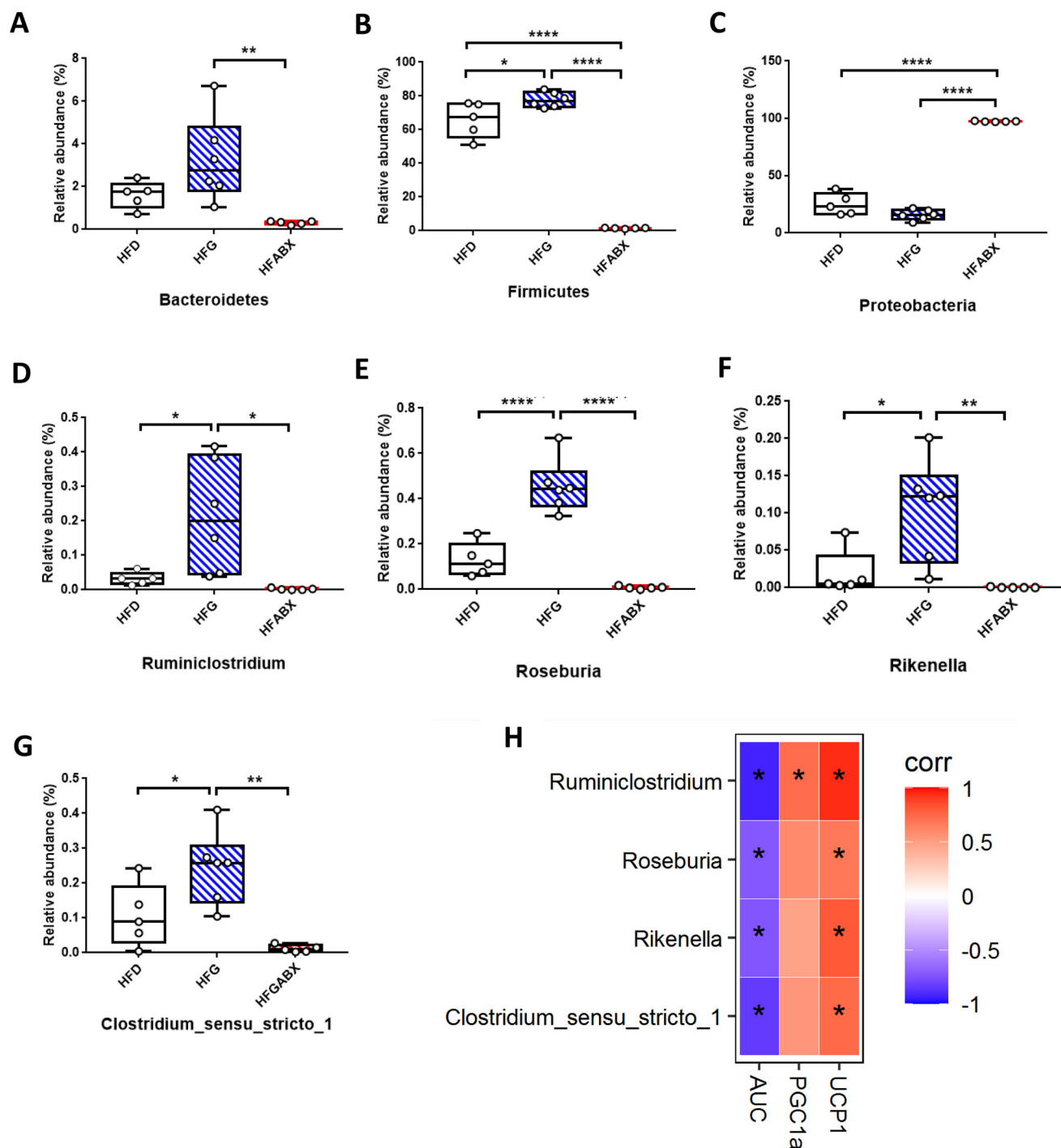


**Fig. 6** Relative abundance of bacterial taxa at different taxonomic levels and the correlation analysis between these dramatically altered genera and the relative expression of thermogenesis indicators in BAT as well as glucose tolerance in obesity mice. (A) Phylum *Bacteroidetes*; (B) phylum *Firmicutes*; (C) phylum *Proteobacteria*; (D) genus *Ruminiclostridium*; (E) genus *Roseburia*; (F) genus *Rikenella*; (G) genus *Clostridium\_sensu\_stricto\_1*; (H) heatmap of spearman correlation analysis. HFD, high-fat diet with a vehicle; HFG, high-fat diet with genistein; HFABX, high-fat diet with genistein and antibiotic cocktail. AUC, area under the curve of IPGTTs; *UCP1*, uncoupling protein 1; *PGC1α*, peroxisome proliferator-activated receptor gamma coactivator 1- $\alpha$ . The statistics were analyzed by MetaStat or spearman correlation analysis ( $n = 5-6$  per group). Differences with  $P < 0.05$  were considered to be significant. \* $p < 0.05$ , \*\* $p < 0.01$ , \*\*\*\* $p < 0.0001$ .

the AUC of IPGTTs. Similarly, a substantial body of literature has reported that *Roseburia* is negatively associated with T2DM.<sup>60</sup> The demonstrated mechanisms include the stimu-

lation of anti-inflammatory cytokines (such as IL-10 and IL-22) known to restore insulin sensitivity and improve glucose metabolism<sup>61,62</sup> and the inhibition of pro-inflammatory cyto-



kines (for instance, IL-17) that promote inflammation.<sup>63,64</sup> Meanwhile, *Roseburia* is a butyrate producing bacterium and butyrate is also known to possess anti-inflammatory property, reduce gut permeability and sustain epithelial integrity.<sup>65,66</sup> In addition, both *Ruminiclostridium* and *Clostridium\_sensu\_stricto\_1* were also confirmed to be butyrate producers<sup>67–69</sup> and their reduced abundance has been linked to hypertriglyceridemia of human cohorts<sup>70,71</sup> and rodent models.<sup>72</sup> In contrast, an improvement of glucose metabolism by almonds,<sup>73</sup> uridine,<sup>74</sup> casein glycomacropeptide hydrolysate,<sup>75</sup> phosphatidylcholines,<sup>76</sup> green alga *Ulva lactuca* polysaccharide,<sup>77</sup> geraniin,<sup>78</sup> tea water extracts,<sup>79</sup> traditional Chinese medicines *Scutellariae radix* and *Coptidis rhizoma*<sup>57</sup> were all positively correlated with the abundance of these bacterial genera. Although the exact function of *Rikenella* is still unclear, Cai *et al.*<sup>80</sup> found that *Rikenella* was involved in the action of resveratrol in ameliorating the progression of DM. Moreover, our previous studies have proved that maternal dietary genistein negates the harmful effects of maternal high-fat diet on glucose and lipid metabolism in both male and female offspring accompanied by the enrichment of *Rikenella*.<sup>31,32</sup> In this study, we found that the supplementation of genistein subsequently increased the levels of *Ruminiclostridium*, *Rikenella*, *Clostridium\_sensu\_stricto\_1* and *Roseburia*, whereas the beneficial effect was abolished in ABX mice, suggesting that these altered microbiota were required in genistein-mediated glucose metabolic benefits.

It has long been known that WAT and BAT are two types of adipose tissue identified in mammals, the former is responsible for energy storage *via* the synthesis and accumulation of triglycerides, while the latter functions in thermogenesis generating heat through the combustion of nutrients that is uncoupled from ATP production by *UCP1*.<sup>81,82</sup> The newest addition, beige adipose tissue, is scattered within the areas of WAT and could be recruitable to exhibit increased thermogenic abilities and similar features to brown adipocytes upon stimulus, such as  $\beta$ -3 adrenergic receptor agonists and cold stimulation.<sup>83–85</sup> Therefore, the promotion of energy expenditure by inducing white adipocyte browning presents a promising avenue for ameliorating metabolic health. In accordance with this notion, the present study evidenced that genistein-treated mice exhibited higher level of browning markers *UCP1* and *PGC1 $\alpha$*  in inguinal SAT compared with that in normal control diet-fed mice. Moreover, an increasing number of studies have reported that active depots of BAT<sup>86</sup> and obesity in adult humans may be caused by impaired BAT activity.<sup>87</sup> Thus, the activation of the thermogenic program in brown adipocytes might serve as a novel strategy for increasing energy dissipation during the treatment of obesity. Our results indicated that a high-fat diet dramatically lowered the mRNA expression of BAT thermogenesis specific genes *UCP1* and *PGC1 $\alpha$* , which were enhanced by genistein treatment.

The identification of novel endogenous mechanisms to promote BAT activity or WAT browning has pointed at gut microbiota as an important modulator of host metabolic homeostasis and energy balance.<sup>88</sup> The absence of gut microbiota, *via* anti-

biotic treatment or in the germ-free model, impaired the adaptive thermogenic capacity of BAT and WAT.<sup>37</sup> The potential role that gut microbiota played in the adipose tissue browning process was also confirmed in the present study. It is noteworthy that these browning markers in WAT and thermogenesis indicators of BAT were all significantly related with enriched beneficial bacteria in mice of genistein administered groups. Moreover, antibiotic administration abolished these positive genistein-induced effects. This may be a novel mechanism to decipher the effects of genistein on gut microbiota composition and the adipose tissue browning program.

Nevertheless, there are still several limitations in our research. Firstly, future studies are needed to examine and elucidate potential sex-dependent mechanisms of action since only female mice were analyzed in this study. Secondly, we found that the SCFA-producing bacteria might be the critical contributor to metabolic benefits of genistein administration, and the molecular mechanism underlying the role of SCFAs mediating metabolic improvement remains unclear of yet. Furthermore, the gut microbiota composition is complex, and even multiple combinations of antibiotics are unable to deplete the gut microbiota completely. It is possible that the imbalance of gut microbiota could influence host metabolic health. Thus, the isolation of specific probiotic species requires further exploration, and the role of ABX treatment alone is worth to be studied. Lastly, although we found that the thermogenesis program was activated by genistein at the molecular level, this study lacked phenotypic data of energy expenditure. More work focused on this is needed in future work, for example, by analyzing mice body composition, assessing energy expenditure and physical activity.

In conclusion, the present research suggested that 10-week genistein intervention not only improved the glucose metabolism and enhanced adipose tissue browning in mice with a normal control diet, but also compensated for the detrimental effects of a high-fat diet in their obese counterparts. Markedly enriched SCFA-producing bacteria and reduced unfavorable species were responsible for the metabolic benefits of genistein gavage. To the best of our knowledge, this is the first work to reveal the causality between gut microbiota modulation and metabolic benefits and adipose tissue browning of genistein supplementation in mice with or without metabolic disturbance. All in all, we provide a new insight into the microbiota–adipose tissue and metabolic homeostasis axis and offer a novel therapeutic strategy of metabolic disorders involving the modulation of gut microbiota.

## Abbreviations

T2DM	Type 2 diabetes mellitus
ABX	Antibiotic cocktail
WAT	White adipose tissue
BAT	Brown adipose tissue
SAT	Subcutaneous adipose tissue
VAT	Visceral adipose tissue





IPGTTs	Intraperitoneal glucose tolerance tests
AUC	Area under the curve
FFAs	Free fatty acids
TG	Total triglyceride
TC	Total cholesterol
HDL-C	High-density lipoprotein cholesterol
LDL-C	Low-density lipoprotein cholesterol
HOMA-IR	Homeostasis model assessment of insulin resistance
OTUs	Operational taxonomic units
PCoA	Principal coordinate analysis
ANOSIM	Analysis of similarities
LEfSe	Linear discriminant analysis of the effect size
UCP1	Uncoupling protein 1
PGC1 $\alpha$	Peroxisome proliferator-activated receptor gamma coactivator 1-alpha
PPAR $\alpha$	Peroxisome proliferator-activated receptor alpha
PPAR $\gamma$	Peroxisome proliferator-activated receptor gamma
PRDM16	Positive regulatory domain containing 16
SCFA	Short chain fatty acid

## Data availability statement

The datasets presented in this study can be found in online repositories. The name of the repository and accession number can be found below: National Center for Biotechnology Information (NCBI) BioProject, <https://www.ncbi.nlm.nih.gov/bioproject/>, PRJNA852669.

## Author contributions

Conceptualization, S. L. and L. Z.; methodology, S. L.; formal analysis, S. L. and L. Z.; investigation, S. L.; resources, X. X.; writing—original draft preparation, S. L.; writing—review and editing, L. Z.; supervision, X. X.; project administration, Q. Z. and M. Y.; funding acquisition, X. X. All authors have read and agreed to the published version of the manuscript.

## Conflicts of interest

There are no conflicts to declare.

## Acknowledgements

This research was funded by the grants from the Beijing Natural Science Foundation (7202163), National Natural Science Foundation of China (No. 82170854, 81870579, 81870545, 81570715, 81170736), Beijing Municipal Science & Technology Commission (Z201100005520011), National Key Research and Development Program of China (2018YFC2001100), and CAMS Innovation Fund for Medical Sciences (CIFMS2021-1-I2M-002, CIFMS2017-I2M-1-008).

We thank Shanghai Biotree Biomedical Biotechnology Co., Ltd for their technical support with high-throughput sequencing.

## References

- 1 IDF Diabetes Atlas, IDF Diabetes Atlas Eighth, 10 edition, 2021, <https://www.diabetesatlas.org/>.
- 2 J. M. Evans, R. W. Newton, D. A. Ruta, T. M. MacDonald and A. D. Morris, Socio-economic status, obesity and prevalence of Type 1 and Type 2 diabetes mellitus, *Diabetic Med.*, 2000, **17**, 478–480.
- 3 G. Bruno, C. Runzo, P. Cavallo-Perin, F. Merletti, M. Rivetti, S. Pinach, G. Novelli, M. Trovati, F. Cerutti and G. Pagano, Incidence of type 1 and type 2 diabetes in adults aged 30–49 years: the population-based registry in the province of Turin, Italy, *Diabetes Care*, 2005, **28**, 2613–2619.
- 4 N. Holman, B. Young and R. Gadsby, Current prevalence of Type 1 and Type 2 diabetes in adults and children in the UK, *Diabetic Med.*, 2015, **32**, 1119–1120.
- 5 R. M. Liu, R. Dai, Y. Luo and J. H. Xiao, Glucose-lowering and hypolipidemic activities of polysaccharides from *Cordyceps taii* in streptozotocin-induced diabetic mice, *BMC Complementary Altern. Med.*, 2019, **19**, 230.
- 6 S. Barnes, T. G. Peterson and L. Coward, Rationale for the use of genistein-containing soy matrices in chemoprevention trials for breast and prostate cancer, *J. Cell. Biochem. Suppl.*, 1995, **22**, 181–187.
- 7 A. A. Franke, L. J. Custer, C. M. Cerna and K. Narala, Rapid HPLC analysis of dietary phytoestrogens from legumes and from human urine, *Proc. Soc. Exp. Biol. Med.*, 1995, **208**, 18–26.
- 8 S. Yamamoto, T. Sobue, S. Sasaki, M. Kobayashi, Y. Arai, M. Uehara, H. Adlercreutz, S. Watanabe, T. Takahashi, Y. Itoi, Y. Iwase, M. Akabane and S. Tsugane, Validity and reproducibility of a self-administered food-frequency questionnaire to assess isoflavone intake in a Japanese population in comparison with dietary records and blood and urine isoflavones, *J. Nutr.*, 2001, **131**, 2741–2747.
- 9 K. D. Setchell, L. Zimmer-Nechemias, J. Cai and J. E. Heubi, Isoflavone content of infant formulas and the metabolic fate of these phytoestrogens in early life, *Am. J. Clin. Nutr.*, 1998, **68**, 1453s–1461s.
- 10 K. P. Devi, B. Shanmuganathan, A. Manayi, S. F. Nabavi and S. M. Nabavi, Molecular and Therapeutic Targets of Genistein in Alzheimer's Disease, *Mol. Neurobiol.*, 2017, **54**, 7028–7041.
- 11 Y. L. Bi, M. Min, W. Shen and Y. Liu, Genistein induced anticancer effects on pancreatic cancer cell lines involves mitochondrial apoptosis, G(0)/G(1) cell cycle arrest and regulation of STAT3 signalling pathway, *Phytomedicine*, 2018, **39**, 10–16.
- 12 H. Marini, A. Bitto, D. Altavilla, B. P. Burnett, F. Polito, V. Di Stefano, L. Minutoli, M. Atteritano, R. M. Levy, N. Frisina, S. Mazzaferro, A. Frisina, R. D'Anna,



- F. Cancellieri, M. L. Cannata, F. Corrado, C. Lubrano, R. Marini, E. B. Adamo and F. Squadrito, Efficacy of genistein aglycone on some cardiovascular risk factors and homocysteine levels: A follow-up study, *Nutr., Metab. Cardiovasc. Dis.*, 2010, **20**, 332–340.
- 13 E. R. Gilbert and D. Liu, Anti-diabetic functions of soy isoflavone genistein: mechanisms underlying its effects on pancreatic  $\beta$ -cell function, *Food Funct.*, 2013, **4**, 200–212.
  - 14 Y. Liu, J. Li, T. Wang, Y. Wang, L. Zhao and Y. Fang, The effect of genistein on glucose control and insulin sensitivity in postmenopausal women: A meta-analysis, *Maturitas*, 2017, **97**, 44–52.
  - 15 I. Zanella, E. Marrazzo, G. Biasiotto, M. Penza, A. Romani, P. Vignolini, L. Caimi and D. Di Lorenzo, Soy and the soy isoflavone genistein promote adipose tissue development in male mice on a low-fat diet, *Eur. J. Nutr.*, 2015, **54**, 1095–1107.
  - 16 C. L. Lyons and H. M. Roche, Nutritional Modulation of AMPK-Impact upon Metabolic-Inflammation, *Int. J. Mol. Sci.*, 2018, **19**(10), 3092.
  - 17 M. Penza, C. Montani, A. Romani, P. Vignolini, B. Pampaloni, A. Tanini, M. L. Brandi, P. Alonso-Magdalena, A. Nadal, L. Ottobri, O. Parolini, E. Bignotti, S. Calza, A. Maggi, P. G. Grigolato and D. Di Lorenzo, Genistein affects adipose tissue deposition in a dose-dependent and gender-specific manner, *Endocrinology*, 2006, **147**, 5740–5751.
  - 18 B. Ahmed, S. Liu and H. Si, Antiadipogenic Effects and Mechanisms of Combinations of Genistein, Epigallocatechin-3-Gallate, and/or Resveratrol in Preadipocytes, *J. Med. Food*, 2017, **20**, 162–170.
  - 19 S. K. Gupta, S. Dongare, R. Mathur, I. R. Mohanty, S. Srivastava, S. Mathur and T. C. Nag, Genistein ameliorates cardiac inflammation and oxidative stress in streptozotocin-induced diabetic cardiomyopathy in rats, *Mol. Cell. Biochem.*, 2015, **408**, 63–72.
  - 20 N. L. Vanden Braber, I. Novotny Nuñez, L. Bohl, C. Porporatto, F. N. Nazar, M. A. Montenegro and S. G. Correa, Soy genistein administered in soluble chitosan microcapsules maintains antioxidant activity and limits intestinal inflammation, *J. Nutr. Biochem.*, 2018, **62**, 50–58.
  - 21 M. A. Rahman Mazumder and P. Hongprabhas, Genistein as antioxidant and antibrowning agents in in vivo and in vitro: A review, *Biomed. Pharmacother.*, 2016, **82**, 379–392.
  - 22 H. Braxas, M. Raftaf, S. Karimi Hasanabad and M. Asghari Jafarabadi, Effectiveness of Genistein Supplementation on Metabolic Factors and Antioxidant Status in Postmenopausal Women With Type 2 Diabetes Mellitus, *Can. J. Diabetes*, 2019, **43**, 490–497.
  - 23 T. Akiyama, J. Ishida, S. Nakagawa, H. Ogawara, S. Watanabe, N. Itoh, M. Shibuya and Y. Fukami, Genistein, a specific inhibitor of tyrosine-specific protein kinases, *J. Biol. Chem.*, 1987, **262**, 5592–5595.
  - 24 C. Weigt, T. Hertrampf, F. M. Kluxen, U. Flenker, F. Hülsemann, K. H. Fritzemeier and P. Diel, Molecular effects of ER  $\alpha$ - and  $\beta$ -selective agonists on regulation of energy homeostasis in obese female Wistar rats, *Mol. Cell. Endocrinol.*, 2013, **377**, 147–158.
  - 25 Y. Heianza, D. Sun, X. Li, J. A. DiDonato, G. A. Bray, F. M. Sacks and L. Qi, Gut microbiota metabolites, amino acid metabolites and improvements in insulin sensitivity and glucose metabolism: the POUNDS Lost trial, *Gut*, 2019, **68**, 263–270.
  - 26 H. Wu, V. Tremaroli, C. Schmidt, A. Lundqvist, L. M. Olsson, M. Krämer, A. Gummesson, R. Perkins, G. Bergström and F. Bäckhed, The Gut Microbiota in Prediabetes and Diabetes: A Population-Based Cross-Sectional Study, *Cell Metab.*, 2020, **32**, 379–390.
  - 27 G. Yang, J. Wei, P. Liu, Q. Zhang, Y. Tian, G. Hou, L. Meng, Y. Xin and X. Jiang, Role of the gut microbiota in type 2 diabetes and related diseases, *Metabolism*, 2021, **117**, 154712.
  - 28 M. Schoeler and R. Caesar, Dietary lipids, gut microbiota and lipid metabolism, *Rev. Endocr. Metab. Disord.*, 2019, **20**, 461–472.
  - 29 R. Yang, Q. Jia, S. Mehmood, S. Ma and X. Liu, Genistein ameliorates inflammation and insulin resistance through mediation of gut microbiota composition in type 2 diabetic mice, *Eur. J. Nutr.*, 2021, **60**, 2155–2168.
  - 30 L. Zhou, X. Xiao, Q. Zhang, J. Zheng, M. Li, X. Wang, M. Deng, X. Zhai and J. Liu, Gut microbiota might be a crucial factor in deciphering the metabolic benefits of perinatal genistein consumption in dams and adult female offspring, *Food Funct.*, 2019, **10**, 4505–4521.
  - 31 L. Zhou, X. Xiao, Q. Zhang, J. Zheng and M. Deng, Maternal Genistein Intake Mitigates the Deleterious Effects of High-Fat Diet on Glucose and Lipid Metabolism and Modulates Gut Microbiota in Adult Life of Male Mice, *Front. Physiol.*, 2019, **10**, 985.
  - 32 L. Zhou, X. Xiao, Q. Zhang, J. Zheng, M. Li, M. Yu, X. Wang, M. Deng, X. Zhai and R. Li, Improved Glucose and Lipid Metabolism in the Early Life of Female Offspring by Maternal Dietary Genistein Is Associated With Alterations in the Gut Microbiota, *Front. Endocrinol.*, 2018, **9**, 516.
  - 33 B. Palacios-González, A. Vargas-Castillo, L. A. Velázquez-Villegas, S. Vasquez-Reyes, P. López, L. G. Noriega, G. Aleman, C. Tovar-Palacio, I. Torre-Villalvazo, L. J. Yang, A. Zarain-Herzberg, N. Torres and A. R. Tovar, Genistein increases the thermogenic program of subcutaneous WAT and increases energy expenditure in mice, *J. Nutr. Biochem.*, 2019, **68**, 59–68.
  - 34 H. H. Shen, S. Y. Huang, C. W. Kung, S. Y. Chen, Y. F. Chen, P. Y. Cheng, K. K. Lam and Y. M. Lee, Genistein ameliorated obesity accompanied with adipose tissue browning and attenuation of hepatic lipogenesis in ovariectomized rats with high-fat diet, *J. Nutr. Biochem.*, 2019, **67**, 111–122.
  - 35 L. Zhou, X. Xiao, Q. Zhang, J. Zheng, M. Li and M. Deng, A Possible Mechanism: Genistein Improves Metabolism and Induces White Fat Browning Through Modulating



- Hypothalamic Expression of Ucn3, Depp, and Stc1, *Front. Endocrinol.*, 2019, **10**, 478.
- 36 X. Chen, J. Xie, Q. Tan, H. Li, J. Lu and X. Zhang, Genistein improves systemic metabolism and enhances cold resistance by promoting adipose tissue beiging, *Biochem. Biophys. Res. Commun.*, 2021, **558**, 154–160.
  - 37 B. Li, L. Li, M. Li, S. M. Lam, G. Wang, Y. Wu, H. Zhang, C. Niu, X. Zhang, X. Liu, C. Hambly, W. Jin, G. Shui and J. R. Speakman, Microbiota Depletion Impairs Thermogenesis of Brown Adipose Tissue and Browning of White Adipose Tissue, *Cell Rep.*, 2019, **26**, 2720–2737.
  - 38 G. Li, C. Xie, S. Lu, R. G. Nichols, Y. Tian, L. Li, D. Patel, Y. Ma, C. N. Brocker, T. Yan, K. W. Krausz, R. Xiang, O. Gavrilova, A. D. Patterson and F. J. Gonzalez, Intermittent Fasting Promotes White Adipose Browning and Decreases Obesity by Shaping the Gut Microbiota, *Cell Metab.*, 2017, **26**, 672–685.
  - 39 R. M. McClain, E. Wolz, A. Davidovich, J. Edwards and J. Bausch, Reproductive safety studies with genistein in rats, *Food Chem. Toxicol.*, 2007, **45**, 1319–1332.
  - 40 R. Michael McClain, E. Wolz, A. Davidovich, F. Pfannkuch, J. A. Edwards and J. Bausch, Acute, subchronic and chronic safety studies with genistein in rats, *Food Chem. Toxicol.*, 2006, **44**, 56–80.
  - 41 S. Reagan-Shaw, M. Nihal and N. Ahmad, Dose translation from animal to human studies revisited, *FASEB J.*, 2008, **22**, 659–661.
  - 42 J. Zheng, X. Xiao, Q. Zhang, M. Yu, J. Xu and Z. Wang, Maternal high-fat diet modulates hepatic glucose, lipid homeostasis and gene expression in the PPAR pathway in the early life of offspring, *Int. J. Mol. Sci.*, 2014, **15**, 14967–14983.
  - 43 T. Magoč and S. L. Salzberg, FLASH: fast length adjustment of short reads to improve genome assemblies, *Bioinformatics*, 2011, **27**, 2957–2963.
  - 44 A. M. Bolger, M. Lohse and B. Usadel, Trimmomatic: a flexible trimmer for Illumina sequence data, *Bioinformatics*, 2014, **30**, 2114–2120.
  - 45 R. C. Edgar, B. J. Haas, J. C. Clemente, C. Quince and R. Knight, UCHIME improves sensitivity and speed of chimera detection, *Bioinformatics*, 2011, **27**, 2194–2200.
  - 46 R. C. Edgar, UPARSE: highly accurate OTU sequences from microbial amplicon reads, *Nat. Methods*, 2013, **10**, 996–998.
  - 47 E. Bolyen, J. R. Rideout, M. R. Dillon, N. A. Bokulich, C. C. Abnet, G. A. Al-Ghalith, H. Alexander, E. J. Alm, M. Arumugam, F. Asnicar, Y. Bai, J. E. Bisanz, K. Bittinger, A. Brejnrod, C. J. Brislawn, C. T. Brown, B. J. Callahan, A. M. Caraballo-Rodríguez, J. Chase, E. K. Cope, R. Da Silva, C. Diener, P. C. Dorrestein, G. M. Douglas, D. M. Durall, C. Duvallet, C. F. Edwardson, M. Ernst, M. Estaki, J. Fouquier, J. M. Gauglitz, S. M. Gibbons, D. L. Gibson, A. Gonzalez, K. Gorlick, J. Guo, B. Hillmann, S. Holmes, H. Holste, C. Huttenhower, G. A. Huttley, S. Janssen, A. K. Jarmusch, L. Jiang, B. D. Kaehler, K. B. Kang, C. R. Keefe, P. Keim, S. T. Kelley, D. Knights, I. Koester, T. Kosciulek, J. Kreps, M. G. I. Langille, J. Lee, R. Ley, Y. X. Liu, E. Loftfield, C. Lozupone, M. Maher, C. Marotz, B. D. Martin, D. McDonald, L. J. McIver, A. V. Melnik, J. L. Metcalf, S. C. Morgan, J. T. Morton, A. T. Naimey, J. A. Navas-Molina, L. F. Nothias, S. B. Orchanian, T. Pearson, S. L. Peoples, D. Petras, M. L. Preuss, E. Pruesse, L. B. Rasmussen, A. Rivers, M. S. Robeson 2nd, P. Rosenthal, N. Segata, M. Shaffer, A. Shiffer, R. Sinha, S. J. Song, J. R. Spear, A. D. Swofford, L. R. Thompson, P. J. Torres, P. Trinh, A. Tripathi, P. J. Turnbaugh, S. Ul-Hasan, J. J. J. van der Hooft, F. Vargas, Y. Vázquez-Baeza, E. Vogtmann, M. von Hippel, W. Walters, Y. Wan, M. Wang, J. Warren, K. C. Weber, C. H. D. Williamson, A. D. Willis, Z. Z. Xu, J. R. Zaneveld, Y. Zhang, Q. Zhu, R. Knight and J. G. Caporaso, Reproducible, interactive, scalable and extensible microbiome data science using QIIME 2, *Nat. Biotechnol.*, 2019, **37**, 852–857.
  - 48 Q. Wang, G. M. Garrity, J. M. Tiedje and J. R. Cole, Naive Bayesian classifier for rapid assignment of rRNA sequences into the new bacterial taxonomy, *Appl. Environ. Microbiol.*, 2007, **73**, 5261–5267.
  - 49 B. H. Goodpaster and L. M. Sparks, Metabolic Flexibility in Health and Disease, *Cell Metab.*, 2017, **25**, 1027–1036.
  - 50 M. Chondronikola, The role of brown adipose tissue and the thermogenic adipocytes in glucose metabolism: recent advances and open questions, *Curr. Opin. Clin. Nutr. Metab. Care*, 2020, **23**, 282–287.
  - 51 X. Liu, B. Mao, J. Gu, J. Wu, S. Cui, G. Wang, J. Zhao, H. Zhang and W. Chen, Blautia—a new functional genus with potential probiotic properties?, *Gut Microbes*, 2021, **13**, 1–21.
  - 52 I. Kimura, K. Ozawa, D. Inoue, T. Imamura, K. Kimura, T. Maeda, K. Terasawa, D. Kashiwara, K. Hirano, T. Tani, T. Takahashi, S. Miyauchi, G. Shioi, H. Inoue and G. Tsujimoto, The gut microbiota suppresses insulin-mediated fat accumulation via the short-chain fatty acid receptor GPR43, *Nat. Commun.*, 2013, **4**, 1829.
  - 53 R. Inoue, R. Ohue-Kitano, T. Tsukahara, M. Tanaka, S. Masuda, T. Inoue, H. Yamakage, T. Kusakabe, K. Hasegawa, A. Shimatsu and N. Satoh-Asahara, Prediction of functional profiles of gut microbiota from 16S rRNA metagenomic data provides a more robust evaluation of gut dysbiosis occurring in Japanese type 2 diabetic patients, *J. Clin. Biochem. Nutr.*, 2017, **61**, 217–221.
  - 54 X. Zhang, Y. Zhao, J. Xu, Z. Xue, M. Zhang, X. Pang, X. Zhang and L. Zhao, Modulation of gut microbiota by berberine and metformin during the treatment of high-fat diet-induced obesity in rats, *Sci. Rep.*, 2015, **5**, 14405.
  - 55 R. S. Thompson, M. Gaffney, S. Hopkins, T. Kelley, A. Gonzalez, S. J. Bowers, M. H. Vitaterna, F. W. Turek, C. L. Foss, C. A. Lowry, F. Vargas, P. C. Dorrestein, K. P. Wright Jr., R. Knight and M. Fleshner, Ruminoclostridium 5, Parabacteroides distasonis, and bile acid profile are modulated by prebiotic diet and associate with facilitated sleep/clock realignment after chronic disruption of rhythms, *Brain, Behav., Immun.*, 2021, **97**, 150–166.



- 56 H. Song, X. Shen, Q. Chu and X. Zheng, Vaccinium bracteatum Thunb. fruit extract reduces high-fat diet-induced obesity with modulation of the gut microbiota in obese mice, *J. Food Biochem.*, 2021, **45**, e13808.
- 57 S. Xiao, C. Liu, M. Chen, J. Zou, Z. Zhang, X. Cui, S. Jiang, E. Shang, D. Qian and J. Duan, Scutellariae radix and coptidis rhizoma ameliorate glycolipid metabolism of type 2 diabetic rats by modulating gut microbiota and its metabolites, *Appl. Microbiol. Biotechnol.*, 2020, **104**, 303–317.
- 58 L. Xiao, B. Chen, D. Feng, T. Yang, T. Li and J. Chen, TLR4 May Be Involved in the Regulation of Colonic Mucosal Microbiota by Vitamin A, *Front. Microbiol.*, 2019, **10**, 268.
- 59 X. Shao, C. Sun, X. Tang, X. Zhang, D. Han, S. Liang, R. Qu, X. Hui, Y. Shan, L. Hu, H. Fang, H. Zhang, X. Wu and C. Chen, Anti-Inflammatory and Intestinal Microbiota Modulation Properties of Jinxiang Garlic (*Allium sativum* L.) Polysaccharides toward Dextran Sodium Sulfate-Induced Colitis, *J. Agric. Food Chem.*, 2020, **68**, 12295–12309.
- 60 M. Gurung, Z. Li, H. You, R. Rodrigues, D. B. Jump, A. Morgun and N. Shulzhenko, Role of gut microbiota in type 2 diabetes pathophysiology, *EBioMedicine*, 2020, **51**, 102590.
- 61 Z. Shen, C. Zhu, Y. Quan, J. Yang, W. Yuan, Z. Yang, S. Wu, W. Luo, B. Tan and X. Wang, Insights into Roseburia intestinalis which alleviates experimental colitis pathology by inducing anti-inflammatory responses, *J. Gastroenterol. Hepatol.*, 2018, **33**, 1751–1760.
- 62 X. Wang, N. Ota, P. Manzanillo, L. Kates, J. Zavala-Solorio, C. Eidenschenk, J. Zhang, J. Lesch, W. P. Lee, J. Ross, L. Diehl, N. van Bruggen, G. Kolumam and W. Ouyang, Interleukin-22 alleviates metabolic disorders and restores mucosal immunity in diabetes, *Nature*, 2014, **514**, 237–241.
- 63 C. Zhu, K. Song, Z. Shen, Y. Quan, B. Tan, W. Luo, S. Wu, K. Tang, Z. Yang and X. Wang, Roseburia intestinalis inhibits interleukin-17 excretion and promotes regulatory T cells differentiation in colitis, *Mol. Med. Rep.*, 2018, **17**, 7567–7574.
- 64 T. W. Hoffmann, H. P. Pham, C. Bridonneau, C. Aubry, B. Lamas, C. Martin-Gallausiaux, M. Moroldo, D. Rainteau, N. Lapaque, A. Six, M. L. Richard, E. Fargier, M. E. Le Guern, P. Langella and H. Sokol, Microorganisms linked to inflammatory bowel disease-associated dysbiosis differentially impact host physiology in gnotobiotic mice, *ISME J.*, 2016, **10**, 460–477.
- 65 M. S. Inan, R. J. Rasoulpour, L. Yin, A. K. Hubbard, D. W. Rosenberg and C. Giardina, The luminal short-chain fatty acid butyrate modulates NF-kappaB activity in a human colonic epithelial cell line, *Gastroenterology*, 2000, **118**, 724–734.
- 66 M. Kinoshita, Y. Suzuki and Y. Saito, Butyrate reduces colonic paracellular permeability by enhancing PPARgamma activation, *Biochem. Biophys. Res. Commun.*, 2002, **293**, 827–831.
- 67 C. C. Evans, K. J. LePard, J. W. Kwak, M. C. Stancukas, S. Laskowski, J. Dougherty, L. Moulton, A. Glawe, Y. Wang, V. Leone, D. A. Antonopoulos, D. Smith, E. B. Chang and M. J. Ciancio, Exercise prevents weight gain and alters the gut microbiota in a mouse model of high fat diet-induced obesity, *PLoS One*, 2014, **9**, e92193.
- 68 O. Appert, A. R. Garcia, R. Frei, C. Roduit, F. Constancias, V. Neuzil-Bunesova, R. Ferstl, J. Zhang, C. Akdis, R. Lauener, C. Lacroix and C. Schwab, Initial butyrate producers during infant gut microbiota development are endospore formers, *Environ. Microbiol.*, 2020, **22**, 3909–3921.
- 69 M. Vital, A. Karch and D. H. Pieper, Colonic Butyrate-Producing Communities in Humans: an Overview Using Omics Data, *mSystems*, 2017, **2**(6), e00130-17.
- 70 G. Maskarinec, P. Raquinio, B. S. Kristal, V. W. Setiawan, L. R. Wilkens, A. A. Franke, U. Lim, L. Le Marchand, T. W. Randolph, J. W. Lampe and M. A. J. Hullar, The gut microbiome and type 2 diabetes status in the Multiethnic Cohort, *PLoS One*, 2021, **16**, e0250855.
- 71 S. Y. Kwan, C. M. Sabotta, A. Joon, P. Wei, L. E. Petty, J. E. Below, X. Wu, J. Zhang, R. R. Jenq, E. T. Hawk, J. B. McCormick, S. P. Fisher-Hoch and L. Beretta, Gut Microbiome Alterations Associated with Diabetes in Mexican Americans in South Texas, *mSystems*, 2022, e0003322, DOI: [10.1128/msystems.00033-22](https://doi.org/10.1128/msystems.00033-22).
- 72 C. Huang, J. Chen, J. Wang, H. Zhou, Y. Lu, L. Lou, J. Zheng, L. Tian, X. Wang, Z. Cao and Y. Zeng, Dysbiosis of Intestinal Microbiota and Decreased Antimicrobial Peptide Level in Paneth Cells during Hypertriglyceridemia-Related Acute Necrotizing Pancreatitis in Rats, *Front. Microbiol.*, 2017, **8**, 776.
- 73 J. M. Choo, C. D. Tran, N. D. Luscombe-Marsh, W. Stonehouse, J. Bowen, N. Johnson, C. H. Thompson, E. J. Watson, G. D. Brinkworth and G. B. Rogers, Almond consumption affects fecal microbiota composition, stool pH, and stool moisture in overweight and obese adults with elevated fasting blood glucose: A randomized controlled trial, *Nutr. Res.*, 2021, **85**, 47–59.
- 74 Y. Liu, C. Xie, Z. Zhai, Z. Y. Deng, H. R. De Jonge, X. Wu and Z. Ruan, Uridine attenuates obesity, ameliorates hepatic lipid accumulation and modifies the gut microbiota composition in mice fed with a high-fat diet, *Food Funct.*, 2021, **12**, 1829–1840.
- 75 Q. Yuan, B. Zhan, R. Chang, M. Du and X. Mao, Antidiabetic Effect of Casein Glycomacropeptide Hydrolysates on High-Fat Diet and STZ-Induced Diabetic Mice via Regulating Insulin Signaling in Skeletal Muscle and Modulating Gut Microbiota, *Nutrients*, 2020, **12**(1), 220.
- 76 X. Gao, L. Du, E. Randell, H. Zhang, K. Li and D. Li, Effect of different phosphatidylcholines on high fat diet-induced insulin resistance in mice, *Food Funct.*, 2021, **12**, 1516–1528.
- 77 Y. Chen, Y. Ouyang, X. Chen, R. Chen, Q. Ruan, M. A. Farag, X. Chen and C. Zhao, Hypoglycaemic and anti-ageing activities of green alga *Ulva lactuca* polysaccharide via gut microbiota in ageing-associated diabetic mice, *Int. J. Biol. Macromol.*, 2022, **212**, 97–110.





- 78 M. Moorthy, C. C. Wie, E. Mariño and U. D. Palanisamy, The Prebiotic Potential of Geraniin and Geraniin-Enriched Extract against High-Fat-Diet-Induced Metabolic Syndrome in Sprague Dawley Rats, *Antioxidants*, 2022, **11**(4), 632.
- 79 J. Liu, W. Hao, Z. He, E. Kwek, Y. Zhao, H. Zhu, N. Liang, K. Y. Ma, L. Lei, W. S. He and Z. Y. Chen, Beneficial effects of tea water extracts on the body weight and gut microbiota in C57BL/6J mice fed with a high-fat diet, *Food Funct.*, 2019, **10**, 2847–2860.
- 80 T. T. Cai, X. L. Ye, R. R. Li, H. Chen, Y. Y. Wang, H. J. Yong, M. L. Pan, W. Lu, Y. Tang, H. Miao, A. M. Snijders, J. H. Mao, X. Y. Liu, Y. B. Lu and D. F. Ding, Resveratrol Modulates the Gut Microbiota and Inflammation to Protect Against Diabetic Nephropathy in Mice, *Front. Pharmacol.*, 2020, **11**, 1249.
- 81 M. E. Vázquez-Vela, N. Torres and A. R. Tovar, White adipose tissue as endocrine organ and its role in obesity, *Arch. Med. Res.*, 2008, **39**, 715–728.
- 82 K. L. Marlatt and E. Ravussin, Brown Adipose Tissue: an Update on Recent Findings, *Curr. Obes. Rep.*, 2017, **6**, 389–396.
- 83 J. Wu, P. Boström, L. M. Sparks, L. Ye, J. H. Choi, A. H. Giang, M. Khandekar, K. A. Virtanen, P. Nuutila, G. Schaart, K. Huang, H. Tu, W. D. van Marken Lichtenbelt, J. Hoeks, S. Enerbäck, P. Schrauwen and B. M. Spiegelman, Beige adipocytes are a distinct type of thermogenic fat cell in mouse and human, *Cell*, 2012, **150**, 366–376.
- 84 J. Wu, P. Cohen and B. M. Spiegelman, Adaptive thermogenesis in adipocytes: is beige the new brown?, *Genes Dev.*, 2013, **27**, 234–250.
- 85 V. Peirce, S. Carobbio and A. Vidal-Puig, The different shades of fat, *Nature*, 2014, **510**, 76–83.
- 86 A. M. Cypess, S. Lehman, G. Williams, I. Tal, D. Rodman, A. B. Goldfine, F. C. Kuo, E. L. Palmer, Y. H. Tseng, A. Doria, G. M. Kolodny and C. R. Kahn, Identification and importance of brown adipose tissue in adult humans, *N. Engl. J. Med.*, 2009, **360**, 1509–1517.
- 87 J. R. Speakman, Evolutionary perspectives on the obesity epidemic: adaptive, maladaptive, and neutral viewpoints, *Annu. Rev. Nutr.*, 2013, **33**, 289–317.
- 88 J. M. Moreno-Navarrete and J. M. Fernandez-Real, The gut microbiota modulates both browning of white adipose tissue and the activity of brown adipose tissue, *Rev. Endocr. Metab. Disord.*, 2019, **20**, 387–397.

